Available online at www.sciencedirect.com

ScienceDirect

Current Opinion in Electrochemistry

Review Article

Electrochemical hydrogenation of NO and CO: Differences and similarities from a computational standpoint

Federico Calle-Vallejo[a,b]

Abstract

Electrolyzers can help in restoring the balance to the biogeochemical cycles of carbon and nitrogen while producing valuable chemical compounds. Before that happens on a global scale, various hurdles need to be overcome, some of which are related to the activity and selectivity of the materials used to catalyze electrolysis reactions. For instance, CO and NO are important electrolysis feedstocks and/or reaction intermediates and their hydrogenation is often energetically demanding. Here it is shown how the most favorable hydrogenation product among *CHO or *COH, and *NHO or *NOH on late transition metals can be ascertained by classification methods based on adsorption-energy scaling relations and "catalytic matrices". In particular, late transition metals can be split into weak-binding and strong-binding and there is a noble-nonnoble energy gap between them. Such a simple categorization helps outline the metals and facets that selectively favor the making of O–H, C–H and N–H bonds.

Addresses

[a] Nano-Bio Spectroscopy Group and European Theoretical Spectroscopy Facility (ETSF), Department of Polymers and Advanced Materials: Physics, Chemistry and Technology, University of the Basque Country UPV/EHU, Avenida Tolosa 72, 20018 San Sebastián, Spain

[b] IKERBASQUE, Basque Foundation for Science, Plaza de Euskadi 5, 48009 Bilbao, Spain

Corresponding author: Calle-Vallejo, Federico (federico.calle@ehu.es)

Current Opinion in Electrochemistry 2023, **42**:101409

This review comes from a themed issue on **Fundamental and Theoretical Electrochemistry (2024)**

Edited by **Kai S. Exner**

For complete overview about the section, refer Fundamental and Theoretical Electrochemistry (2024)

Available online 13 October 2023

https://doi.org/10.1016/j.coelec.2023.101409

Keywords

NO hydrogenation, CO hydrogenation, Scaling relation, Catalytic matrix, Classification method, Late transition metal.

Introduction

After more than a decade of focalized research on CO_2 reduction and akin reactions within the carbon cycle [1–4], some electroreduction reactions belonging to the nitrogen cycle are regaining considerable attention [5–9]. This is a timely diversification of the research efforts, as the imbalance of the nitrogen cycle is larger than that of the carbon cycle but far less publicized to this date [10]. In this new wave of nitrogen electrocatalysis it is worth noting that some authors have called for and put forward rigorous experimental protocols for product detection and quantification of reaction products, with the aim of enabling one-to-one comparisons across different laboratories [11–13]. In addition, the co-electrolysis of oxidized C- and N-containing species is an appealing, low-temperature route toward urea and other compounds with C–N bonds, which can help in reaching the much-needed but arduous rebalance of both biogeochemical cycles [4,14–18].

Because CO hydrogenation and NO hydrogenation are both energy-intensive and impact the overall performance of catalysts for CO and NO electroreduction [19–25], it is useful to compare the trends among various materials to establish key differences and similarities. Specifically, it is of great interest for the rational design of electrocatalysts to ascertain whether a given active site drives *CO hydrogenation toward *CHO or *COH, and whether it drives *NO hydrogenation toward *NHO or *NOH (here, an asterisk next to a species indicates that the species is adsorbed), following the reactions shown below.

$$*CO + H^+ + e^- \rightarrow *COH \quad (1)$$

$$*CO + H^+ + e^- \rightarrow *CHO \quad (2)$$

$$*NO + H^+ + e^- \rightarrow *NOH \quad (3)$$

$$*NO + H^+ + e^- \rightarrow *NHO \quad (4)$$

Establishing general trends in the selectivity of materials toward those four electrochemical steps is useful for the following reasons:

- It is still widely believed that *CO hydrogenation most often leads to *CHO, and that the persistent scaling relation between those two species is responsible for the large overpotentials of CO and CO_2 electroreduction to methane [23,26].
- It is not yet clear when *NO hydrogenation leads to *NHO or *NOH on late transition metals, and factors such as electrode composition and morphology, and adsorbate coverage seem to play a role [20,21,25,27,28].
- Co-electrolysis pathways to urea may involve *NO, *CO and their most favorable hydrogenated counterparts [16–18].
- It is a widespread practice to represent polycrystalline electrodes and nanoparticles by means of a single surface site, often located at (111) terraces.

As I think that the classifications based on adsorption energies and the scaling relations thereof put forward by Bagger, Rossmeisl and coworkers are intuitive and insightful [9,16,25,29–31], I provide in the following a comparison of *NO and *CO hydrogenation on late transition metals along similar lines and supplement the observations by the structure-sensitive insights of "catalytic matrices" [22,27]. Detailed analyses toward various final products are available elsewhere [9,21,23,32].

My aim is not to connect the selectivity of *CO or *NO hydrogenation with the product distribution of their overall reduction reactions. Indeed, the C_1 vs C_2 selectivity of CO electroreduction depends on whether *CO is dimerized or hydrogenated, and the ethylene/ethanol selectivity depends on the product of $*CH_2CHO$ hydrogenation [33,34]. I aim to show that *NO and *CO hydrogenations may generally be energy-intensive and potential-limiting. Enhancing their electrocatalysis entails stabilizing the hydrogenation products of *NO and *CO. Because the geometric and electronic structures, adsorption configurations and solvent-adsorbate interactions of *NHO and *NOH are different and the same applies to *CHO and *COH, it is paramount to ascertain the one formed depending on the catalyst structure and reaction conditions.

Trends in CO and NO hydrogenation on late transition metals

The following analysis is based on thermodynamic considerations. The adsorption energies of *CO, *CHO, *COH [22], *NO, *NHO and *NOH [27] on Co, Ni, Cu, Rh, Pd, Ag, Ir, Pt, and Au were assessed by means of density functional theory (DFT) calculations, see Table S1. Both datasets were produced with VASP [35], making use of the PBE functional [36] and the PAW method [37]. The free energies are based on the DFT total energy (E_{DFT}), the zero-point energy (ZPE) and include entropic corrections (TS) and adsorbate-solvent stabilization corrections (E_{solv}): $G \approx E_{DFT} + ZPE - TS + E_{solv}$. The adsorption energies are defined with respect to $CO(g)$, $NO(g)$, and $(H^+ + e^-)$. The total energies of $CO(g)$ and $NO(g)$ include gas-phase corrections [38–40], which ensure that the reaction energies and equilibrium potentials agree with experiments. The energetics of $(H^+ + e^-)$ is calculated using the computational hydrogen electrode [41]. Metal-independent adsorbate-solvent interaction corrections were added to the adsorption energies of *CO, *CHO and *COH (−0.10, −0.10, −0.38 eV) [22,33], while metal-, facet-, and adsorbate-specific corrections obtained using an iterative micro-solvation method were added to the adsorption energies of *NO, *NHO and *NOH [27,42,43].

Before continuing, I stress that incorporating or neglecting the aforementioned gas-phase and adsorbate-solvent corrections may substantially affect the predictiveness of computational models. For instance, significant differences between the slopes and offsets of scaling relations in vacuum and with an implicit solvent have been shown for metalloporphyrins [44]. That activity trends remain untouched in spite of the DFT errors present in the calculations used to establish them is an extended, widely accepted yet inaccurate perception [38,42,45].

Of course, other effects such as reaction kinetics, adsorbate coverage, bulk and local pH, mass transport, cation effects, electrode potential, etc. [1,2,11,20,46–49] also ought to be incorporated into computational electrocatalysis models, preferably in simple terms. For example, previous works showed that the adsorption energies of species under an electric field may undergo sizeable shifts depending on the magnitude and sign of the field, and the polarizability and dipole moment of the adsorbates [50]. Hence, adsorption-energy scaling relations might be appreciably modified under electrochemical conditions. Besides, high adsorbate coverages modify scaling relations [51,52] and have a direct impact on the reaction pathway, voltametric profile and catalytic activity of Pt(111) and Pt(100) for NO electroreduction [20,28].

The adsorption sites considered here comprise terraces ((111) and (100)), steps ((211) and (211) kinked), and metal adatoms (3AD @ (111)), as schematized in Figure S1. Those adsorption sites span a range of coordination numbers (cn) between 5 and 9. A disclaimer is necessary here: the offsets of adsorption-energy scaling relations on metals tend to vary as a function of cn, except when the slope is unity (or $^3/_4$ for C-bound species) [32,53,54]. Here, however, to simplify the

analysis, I made a single linear fit for all datapoints, which comes at the expense of increasing the mean absolute errors (MAEs) and decreasing the correlation coefficients (r). Anyway, the MAEs in Figures 1–4 are below 0.20 eV, and r is larger than 0.90 in all cases.

Classifications based on scaling relations

According to Figure 1a–b, there exist adsorption-energy scaling relations [53,55] between *CHO, *COH, and *CO, and between *NHO, *NOH and *NO. Figure 1c shows that *NO and *CO also scale. Thus, Figure 1 indicates that, within certain accuracy, all six adsorbates scale with each other, such that linear co-electrolysis models based on a reduced number of parameters are possible [16]. However, the appreciably different fits in Figure 1a–b attest to specific binding differences. In particular, the slope of the *CHO vs. *CO relation is ≈1 and that of *COH vs. *CO is ≈3/2. These values suggest that the valency of *CHO and *CO is nearly identical, whereas that of *COH and *CO differs by one [22]. For *NHO vs. *NO the slope is between $^1/_2$ and 1, and close to 1 for *NOH vs. *NO [27]. In addition, the slope of *CO vs *NO in Figure 1c is also in the range of $^1/_2$ and 1, which is indicative of their different valency. In sum, the slopes are in the approximate range between 1/2 and 3/2, and it is

Figure 1

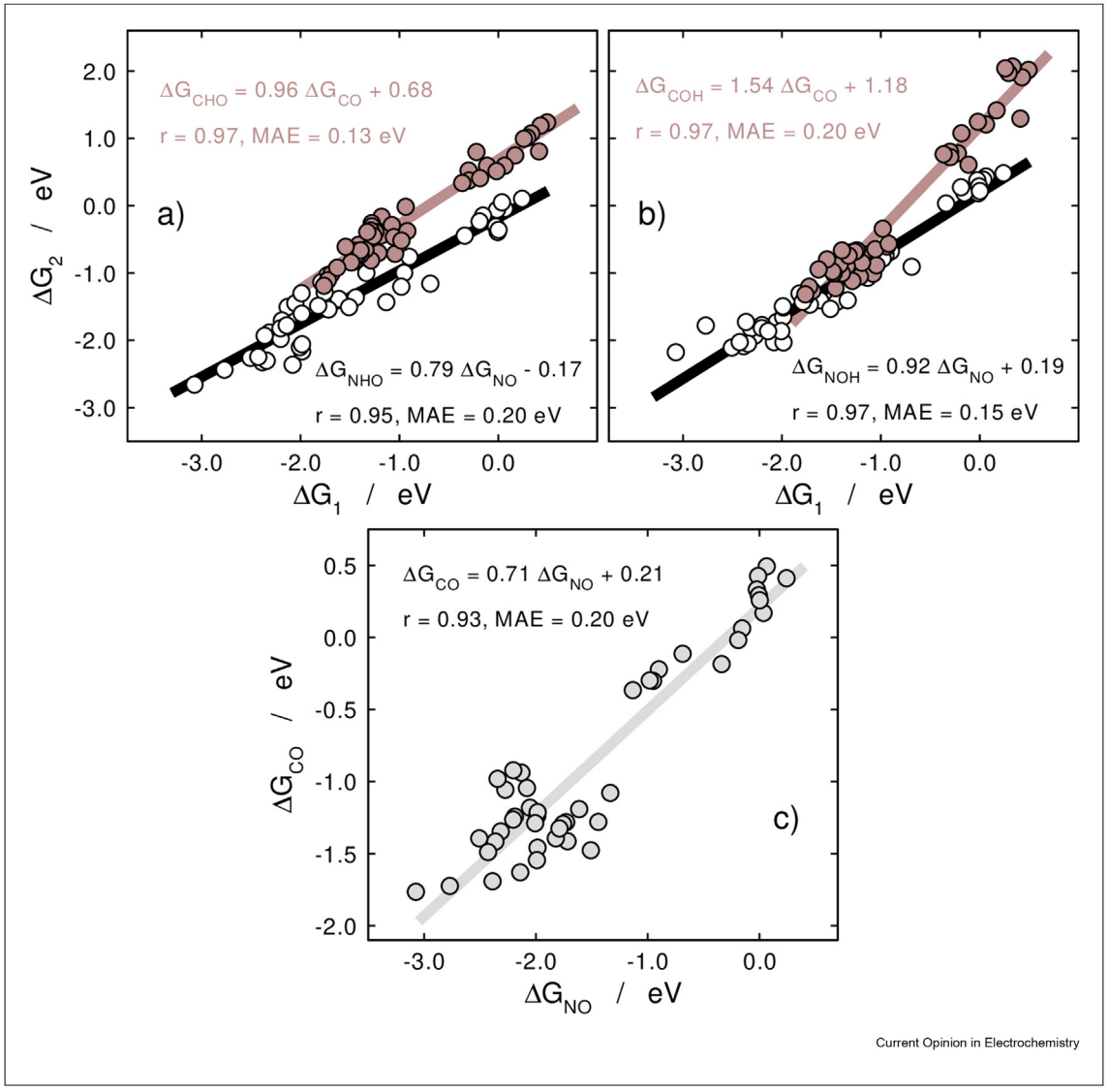

Adsorption-energy scaling relations among C- and N-containing species. a) *CHO vs *CO, and *NHO vs. *NO. b) *COH vs. *CO, and *NOH vs. *NO. c) *CO vs. *NO. In each case, the least-squares linear fit, correlation coefficient (r) and mean absolute error (*MAE*) are provided. The adsorption energies in this figure were taken from previous works [22,27] and appear in Table S1.

Figure 2

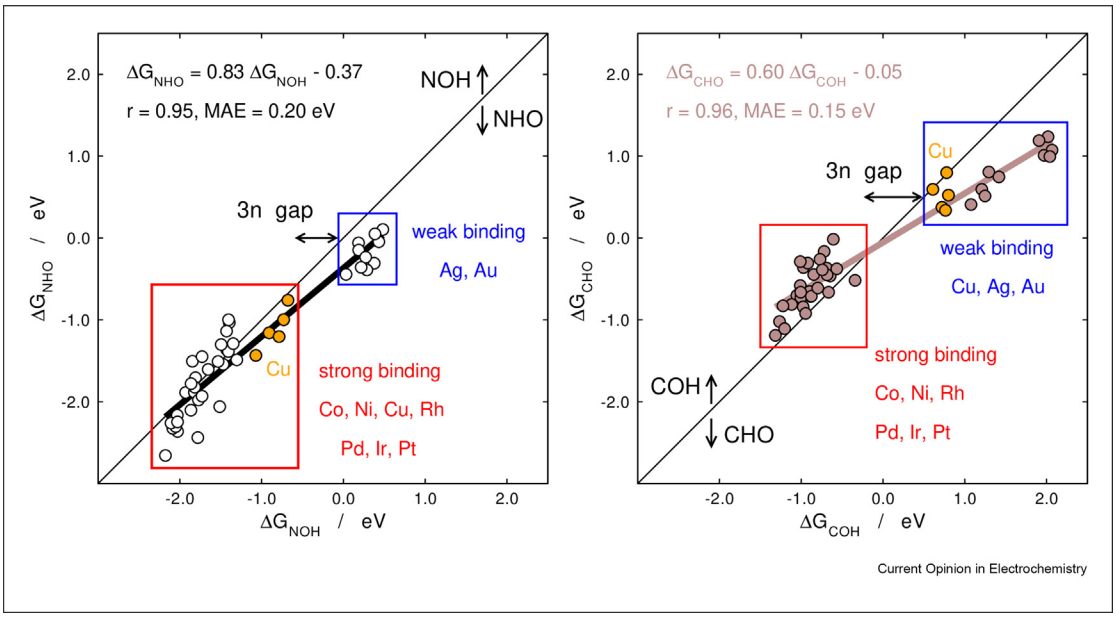

Selectivity of *NO hydrogenation (left) and *CO hydrogenation (right), as described by the combination of scaling relations and a parity line. Active sites above the parity line are thermodynamically inclined to produce *NOH and *COH, while those below produce *NHO and *CHO. In each case, the least-squares linear fit, correlation coefficient (*r*) and mean absolute error (*MAE*) are provided. The adsorption energies were taken from previous works [22,27] and appear in Table S1.

Figure 3

metal / facet	111 cn = 9	100 cn = 8	211 cn = 7	211k cn = 6	3AD@111 cn = 5
Co	COH	COH	COH	COH	CHO
Rh	COH	COH	COH	COH	COH
Ir	COH	COH	COH	both (COH)	COH
Ni	COH	COH	COH	COH	both (COH)
Pd	COH	COH	COH	COH	COH
Pt	COH	COH	COH	COH	both (COH)
Cu	both (COH)	both (CHO)	CHO	CHO	CHO
Ag	CHO	CHO	CHO	CHO	CHO
Au	CHO	CHO	CHO	CHO	CHO

metal / facet	111 cn = 9	100 cn = 8	211 cn = 7	211k cn = 6	3AD@111 cn = 5
Co	NOH	NHO	both (NOH)	NHO	NHO
Rh	both (NOH)	NHO	both (NHO)	NHO	NHO
Ir	both (NOH)	NHO	NHO	NHO	NHO
Ni	NOH	NHO	NOH	both (NHO)	NHO
Pd	NOH	both (NOH)	both (NOH)	NOH	NOH
Pt	NOH	both (NHO)	NHO	both (NOH)	both (NOH)
Cu	both (NHO)	NHO	NHO	NHO	NHO
Ag	NHO	NHO	NHO	NHO	NHO
Au	NHO	NHO	NHO	NHO	NHO

Current Opinion in Electrochemistry

Catalytic matrices for *CO hydrogenation (left) and *NO hydrogenation (right) on nine late transition metals and five surface facets. Sites for which $abs(\Delta G_{NOH} - \Delta G_{NHO})$<0.1 *eV* and $abs(\Delta G_{COH} - \Delta G_{CHO})$<0.1 *eV* are referred to as "both" and their slight preference is indicated. Left: reprinted (adapted) with permission from Ref. [22], copyright 2017 American Chemical Society. Right: replotted from Ref. [27], licensed under CC BY 4.0 (https://creativecommons.org/licenses/by/4.0/).

interesting that the relationships with a slope close to unity are *CHO vs. *CO and *NOH vs. *NO.

The classifications by Bagger, Rossmeisl and coworkers are usually based on a vertical line that intersects a horizontal one. The lines are not arbitrarily set but rather correspond to equilibrium adsorption energies. Metals to the left or below the lines bind strongly, whereas those to the right or above the lines bind weakly. Figure S2 shows that the positions of the metals

Figure 4

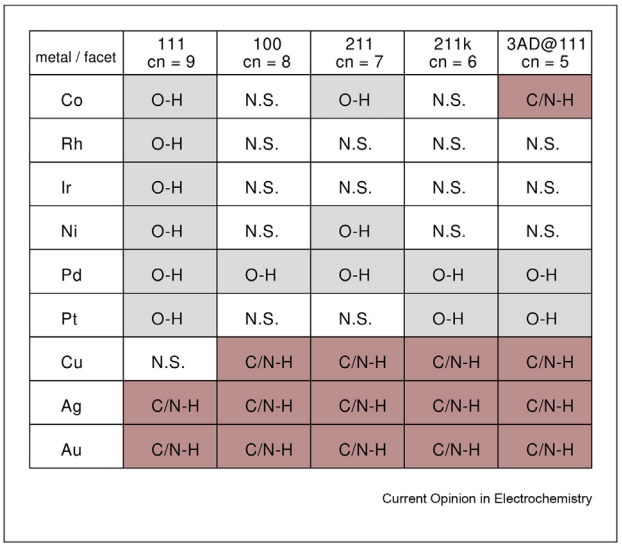

metal / facet	111 cn = 9	100 cn = 8	211 cn = 7	211k cn = 6	3AD@111 cn = 5
Co	O-H	N.S.	O-H	N.S.	C/N-H
Rh	O-H	N.S.	N.S.	N.S.	N.S.
Ir	O-H	N.S.	N.S.	N.S.	N.S.
Ni	O-H	N.S.	O-H	N.S.	N.S.
Pd	O-H	O-H	O-H	O-H	O-H
Pt	O-H	N.S.	N.S.	O-H	O-H
Cu	N.S.	C/N-H	C/N-H	C/N-H	C/N-H
Ag	C/N-H	C/N-H	C/N-H	C/N-H	C/N-H
Au	C/N-H	C/N-H	C/N-H	C/N-H	C/N-H

Current Opinion in Electrochemistry

Catalytic matrix illustrating the preference of various active sites on transition metals upon hydrogenation. O–H: active sites inclined toward the formation of O–H bonds. C/N–H: active sites inclined toward the formation of C–H and N–H bonds. N.S.: Not selective, namely, active sites that may indistinctively form O–H or C–H and N–H bonds.

with respect to the equilibrium binding energies do not play a role in their selectivity toward *NHO/*NOH and *CHO/*COH. Alternatively, overall selectivity trends can be inferred from the intersection of scaling relations and the parity line ($y = x$), as in Figure 2. Datapoints above the parity line correspond to *NOH- and *COH-producing materials, while those below the line are selective to *NHO and *CHO. Both scaling relations in Figure 2 can be divided into two parts: a weak-binding region and a strong-binding region. The two regions are separated by a "noble-nonnoble gap" or "3*n* gap", which is the region between the red and blue rectangles. In it, no materials are observed when analyzing trends for late transition metals. Although I cannot currently justify the existence of such a gap, it can also be noticed in previous works for other C-containing species adsorbed on metals [32] and materials such as single-atom catalysts and metalloporphyrins [56,57]. As the gap tends to be relatively wide, it may facilitate the making of alternative activity and selectivity classifications.

Ag and Au are always in the weak-binding region, whereas Co, Ni, Rh, Pd, Ir and Pt are always in the strong-binding region. Interestingly, Cu switches sides: it is a weak-binding metal for *CO hydrogenation and a strong-binding metal for *NO hydrogenation and is close to the 3*n* gap in both cases. In terms of selectivity, Figure 2 indicates that weak-binding metals are selective to *NHO and *CHO. Conversely, strong-binding metals are selective to *COH but have mixed selectivity toward *NOH and *NHO.

Catalytic matrices

Although scaling relations are rather insightful, there is a limit as to how much they can visually display before a given figure looks cluttered. In such a case, one can resort to "catalytic matrices", which help in identifying structure-sensitive activity and selectivity patterns [22,27]. In those, adsorption-energy datasets are presented as a matrix in which the entries depend on the element and its surface coordination. Moreover, catalytic matrices can be approximated by means of simple multivariate regressions [27].

As shown in Figure 3, catalytic matrices condense all the selectivity data present in the scaling relations of *CHO vs. *COH and *NHO vs. *NOH in an organized manner. I often find valuable the ascertainment of how representative of an entire electrode is a specific facet. For instance, it is common to represent polycrystalline electrodes of fcc metals by their (111) facet, allegedly because it is the most stable one. Catalytic matrices give hints on the suitability of this simplification.

According to Figure 3, (111) terraces are an acceptable qualitative approximation of a polycrystalline electrode for *CO hydrogenation, as the selectivity does not vary strongly as a function of *cn*. This is clear in Figure 2 (right), where the intersection between the parity line and the scaling relation takes place within the 3*n* gap, such that the selectivity depends only on whether a material binds strongly or weakly. However, for *NO hydrogenation this approximation is only advisable for Pd, Cu, Ag, and Au, as the intersection of the parity line and the scaling relation occurs within the red rectangle in Figure 2 (left).

For comparison, the two matrices in Figure 3 are combined in Figure 4, which allows one to extract some overall conclusions for late transition metals. Specifically, Cu, Ag and Au tend to produce species with C–H and N–H bonds (*CHO/*NHO). In turn, Pd is inclined to produce species with O–H bonds (*COH/*NOH). This is also true for the (111) facet of strong-binding metals. For all those specific elements and facets, the trends in *NO and *CO hydrogenation are certainly analogous. Nevertheless, there are various sites in Figure 4 predicted to produce *COH and *NHO and classified as "not selective (N.S.)". Interestingly, no active site in the matrix produces *CHO and *NOH.

Finally, based on Figures 2 and 3, it is not advisable to assume that the preferred hydrogenation product of *CO is always *CHO, as often assumed in the literature [23,26]. In fact, kinetic analyses using single-crystal electrodes have shown that the preference for *CHO or *COH is facet- and potential-dependent on Cu electrodes [46].

Concluding remarks

Scaling relations are one of the cornerstones of contemporary computational electrocatalysis, and catalytic matrices help summarize and analyze large datasets. Both tools are useful in materials screening studies, the accuracy of which might increase if the effects of various parameters are probed, understood and routinely considered. Catalytic matrices should in the future incorporate information on *H, as hydrogen evolution usually competes with numerous electrochemical reactions [25].

Delving into *CO and *NO hydrogenation with the help of these two tools, I conclude that, although those two adsorbates may at first sight seem similar, their adsorption energies and hydrogenation products on late transition metals differ qualitatively and quantitatively. The main features of *NO and *CO hydrogenation from a computational standpoint are:

- *CO and *NO scale linearly but not with a unity slope, so their valency is different. *CO scales with *CHO with a slope close to 1. Conversely, *NO does so with *NOH.
- Late transition metals can be classified into strong- and weak-binding. There is a noble-nonnoble gap (or 3n gap) separating the two groups. Only Cu moves between groups, while Ag and Au are in both cases weak-binding, and Co, Ni, Rh, Pd, Ir and Pt are in both cases strong-binding.
- Catalytic matrices show that the (111) facet of strong-binding metals and all facets of Pd favor O−H bond formation during *NO and *CO hydrogenation. Conversely, Cu, Ag, and Au favor the formation of C−H and N−H bonds.
- Qualitatively, it is fair to assume that the (111) facet of late transition metals approximates well the selectivity of polycrystalline electrodes for *CO hydrogenation. Nevertheless, this is true only for weak-binding metals and Pd for *NO hydrogenation. Except for weak-binding metals, assuming that *CO hydrogenation always leads to *CHO is not a good approximation.

Declaration of competing interest

The author declares that he has no known competing financial interests or personal relationships that could have appeared to influence the work reported in this paper.

Data availability

All the data are provided in the Supplementary Material.

Acknowledgments

This work received financial support from grants PID2021-127957NB-I00 and TED2021-132550B−C21, which are funded by MCIN/AEI/10.13039/501100011033 and by the European Union.

Appendix A. Supplementary data

Supplementary data to this article can be found online at https://doi.org/10.1016/j.coelec.2023.101409.

References

Papers of particular interest, published within the period of review, have been highlighted as:

* of special interest
** of outstanding interest

1. Nitopi S, Bertheussen E, Scott SB, Liu X, Engstfeld AK, Horch S, Seger B, Stephens IEL, Chan K, Hahn C, Nørskov JK, Jaramillo TF, Chorkendorff I: **Progress and perspectives of electrochemical CO2 reduction on copper in aqueous electrolyte**. *Chem Rev* 2019, **119**:7610−7672, https://doi.org/10.1021/acs.chemrev.8b00705.

2. Birdja YY, Pérez-Gallent E, Figueiredo MC, Göttle AJ, Calle-Vallejo F, Koper MTM: **Advances and challenges in understanding the electrocatalytic conversion of carbon dioxide to fuels**. *Nat Energy* 2019, **4**, https://doi.org/10.1038/s41560-019-0450-y.

3. Handoko AD, Wei F, Jenndy, Yeo BS, Seh ZW: **Understanding heterogeneous electrocatalytic carbon dioxide reduction through operando techniques**. *Nat Catal* 2018, **1**:922−934, https://doi.org/10.1038/s41929-018-0182-6.

4. Tang C, Zheng Y, Jaroniec M, Qiao S: **Electrocatalytic refinery for sustainable production of fuels and chemicals**. *Angew Chem Int Ed* 2021, **60**:19572−19590, https://doi.org/10.1002/anie.202101522.

5. van Langevelde PH, Katsounaros I, Koper MTM: **Electrocatalytic nitrate reduction for sustainable ammonia production**. *Joule* 2021, **5**:290−294, https://doi.org/10.1016/j.joule.2020.12.025.

6. Wang Y, Xu A, Wang Z, Huang L, Li J, Li F, Wicks J, Luo M, Nam D, Tan C, Ding Y, Wu J, Lum Y, Dinh C, Sinton D, Zheng G, Sargent EH: **Enhanced nitrate-to-ammonia activity on copper−nickel alloys via tuning of intermediate adsorption**. *J Am Chem Soc* 2020, **142**:5702−5708, https://doi.org/10.1021/jacs.9b13347.

7. McEnaney JM, Blair SJ, Nielander AC, Schwalbe JA, Koshy DM, Cargnello M, Jaramillo TF: **Electrolyte engineering for efficient electrochemical nitrate reduction to ammonia on a titanium electrode**. *ACS Sustainable Chem Eng* 2020, **8**:2672−2681, https://doi.org/10.1021/acssuschemeng.9b05983.

8. Wang M, Khan MA, Mohsin I, Wicks J, Ip AH, Sumon KZ, Dinh C, Sargent EH, Gates ID, Kibria MG: **Can sustainable ammonia synthesis pathways compete with fossil-fuel based Haber−Bosch processes?** *Energy Environ Sci* 2021, **14**:2535−2548, https://doi.org/10.1039/D0EE03808C.

9. Wan H, Bagger A, Rossmeisl J: **Electrochemical nitric oxide reduction on metal surfaces**. *Angew Chem Int Ed* 2021, **60**:21966−21972, https://doi.org/10.1002/anie.202108575.

10. Rockström J, Steffen W, Noone K, Persson Å, Chapin FS, Lambin EF, Lenton TM, Scheffer M, Folke C, Schellnhuber HJ, Nykvist B, de Wit CA, Hughes T, van der Leeuw S, Rodhe H, Sörlin S, Snyder PK, Costanza R, Svedin U, Falkenmark M, Karlberg L, Corell RW, Fabry VJ, Hansen J, Walker B, Liverman D, Richardson K, Crutzen P, Foley JA: **A safe operating space for humanity**. *Nature* 2009, **461**:472−475, https://doi.org/10.1038/461472a.

11. * Katsounaros I: **On the assessment of electrocatalysts for nitrate reduction**. *Curr Opin Electrochem* 2021, **28**, 100721, https://doi.org/10.1016/j.coelec.2021.100721.
Summary of the challenges and pitfalls in experimental nitrate electroreduction. A number of factors may lead to flawed results, which calls for rigorous protocols.

12. Iriawan H, Andersen SZ, Zhang X, Comer BM, Barrio J, Chen P, Medford AJ, Stephens IEL, Chorkendorff I, Shao-Horn Y: **Methods for nitrogen activation by reduction and oxidation**. *Nature Reviews Methods Primers* 2021, **1**:56, https://doi.org/10.1038/s43586-021-00053-y.

13. Andersen SZ, Čolić V, Yang S, Schwalbe JA, Nielander AC, McEnaney JM, Enemark-Rasmussen K, Baker JG, Singh AR, Rohr BA, Statt MJ, Blair SJ, Mezzavilla S, Kibsgaard J, Vesborg PCK, Cargnello M, Bent SF, Jaramillo TF, Stephens IEL, Nørskov JK, Chorkendorff I: **A rigorous electrochemical ammonia synthesis protocol with quantitative isotope measurements**. *Nature* 2019, **570**:504–508, https://doi.org/10.1038/s41586-019-1260-x.

14. Shibata M, Yoshida K, Furuya N: **Electrochemical synthesis of urea at gas-diffusion electrodes: IV. Simultaneous reduction of carbon dioxide and nitrate ions with various metal catalysts**. *J Electrochem Soc* 1998, **145**:2348, https://doi.org/10.1149/1.1838641.

15. Li J, Zhang Y, Kuruvinashetti K, Kornienko N: **Construction of C–N bonds from small-molecule precursors through heterogeneous electrocatalysis**. *Nat Rev Chem* 2022, **6**:303–319, https://doi.org/10.1038/s41570-022-00379-5.

16. ** Wan H, Wang X, Tan L, Filippi M, Strasser P, Rossmeisl J, Bagger A: **Electrochemical synthesis of urea: Co-reduction of nitric oxide and carbon monoxide**. *ACS Catal* 2023, **13**: 1926–1933, https://doi.org/10.1021/acscatal.2c05315.
Urea production from a computational perspective by coupling NO and CO. Apart from classification methods, coupling barriers are calculated and a microkinetic model is provided

17. Jiang M, Zhu M, Wang M, He Y, Luo X, Wu C, Zhang L, Jin Z: **Review on electrocatalytic coreduction of carbon dioxide and nitrogenous species for urea synthesis**. *ACS Nano* 2023, **17**: 3209–3224, https://doi.org/10.1021/acsnano.2c11046.

18. Huang Y, Yang R, Wang C, Meng N, Shi Y, Yu Y, Zhang B: **Direct electrosynthesis of urea from carbon dioxide and nitric oxide**. *ACS Energy Lett* 2022, **7**:284–291, https://doi.org/10.1021/acsenergylett.1c02471.

19. Hori Y, Takahashi R, Yoshinami Y, Murata A: **Electrochemical reduction of CO at a copper electrode**. *J Phys Chem B* 1997, **101**:7075–7081, https://doi.org/10.1021/jp970284i.

20. Katsounaros I, Figueiredo MC, Chen X, Calle-Vallejo F, Koper MTM: **Structure- and coverage-sensitive mechanism of NO reduction on platinum electrodes**. *ACS Catal* 2017, **7**, https://doi.org/10.1021/acscatal.7b01069.

21. ** Casey-Stevens CA, Ásmundsson H, Skúlason E, Garden AL: **A density functional theory study of the mechanism and onset potentials for the major products of NO electroreduction on transition metal catalysts**. *Appl Surf Sci* 2021, **552**, 149063, https://doi.org/10.1016/j.apsusc.2021.149063.
Thorough analysis of NO electroreduction on the fcc (111) and hcp (0001) surfaces of numerous transition metals toward various products

22. * Calle-Vallejo F, Koper MTM: **Accounting for bifurcating pathways in the screening for CO2 reduction catalysts**. *ACS Catal* 2017, **7**, https://doi.org/10.1021/acscatal.7b02917.
Structure-sensitive trends for *CO hydrogenation to *COH and *CHO on late transition metals described using catalytic matrices and scaling relations

23. Peterson AA, Nørskov JK: **Activity descriptors for CO2 electroreduction to methane on transition-metal catalysts**. *J Phys Chem Lett* 2012, **3**:251–258, https://doi.org/10.1021/jz201461p.

24. de Vooys ACA, Koper MTM, van Santen RA, van Veen JAR: **Mechanistic study of the nitric oxide reduction on a polycrystalline platinum electrode**. *Electrochim Acta* 2001, **46**: 923–930, https://doi.org/10.1016/S0013-4686(00)00678-2.

25. ** Bagger A: **Reduction reactions versus hydrogen**. *Curr Opin Electrochem* 2023, **40**, 101339, https://doi.org/10.1016/j.coelec.2023.101339.
Comparison of trends in the selectivity of N_2, NO_x and CO_2 reduction reactions and H_2 evolution by means of intuitive classification methods

26. Li Y, Sun Q: **Recent advances in breaking scaling relations for effective electrochemical conversion of CO2**. *Adv Energy Mater* 2016, **6**, 1600463, https://doi.org/10.1002/aenm.201600463.

27. * Romeo E, Lezana-Muralles M, Illas F, Calle-Vallejo F: **Extracting features of active transition metal electrodes for NO electroreduction with catalytic matrices**. *ACS Appl Mater Interfaces* 2023, **15**:22176–22183, https://doi.org/10.1021/acsami.3c03385.
Structure-sensitive trends for *NO hydrogenation to *NOH and *NHO on late transition metals described using catalytic matrices and scaling relations

28. * Chun H, Apaja V, Clayborne A, Honkala K, Greeley J: **Atomistic insights into nitrogen-cycle electrochemistry: a combined DFT and kinetic Monte Carlo analysis of no electrochemical reduction on Pt(100)**. *ACS Catal* 2017, **7**:3869–3882, https://doi.org/10.1021/acscatal.7b00547.
Thorough computational study of NO electroreduction on Pt(100). Numerous effects (e.g., adsorbate coverage, solvation, reaction kinetics) were incorporated in the model and the resulting voltammograms are in remarkable agreement with previous experiments.

29. Bagger A, Ju W, Varela AS, Strasser P, Rossmeisl J: **Electrochemical CO2 reduction: a classification problem**. *ChemPhysChem* 2017, **18**:3266–3273, https://doi.org/10.1002/cphc.201700736.

30. Bagger A, Ju W, Varela AS, Strasser P, Rossmeisl J: **Electrochemical CO2 reduction: classifying Cu facets**. *ACS Catal* 2019, **9**:7894–7899, https://doi.org/10.1021/acscatal.9b01899.

31. Bagger A, Wan H, Stephens IEL, Rossmeisl J: **Role of catalyst in controlling N2 reduction selectivity: a unified view of nitrogenase and solid electrodes**. *ACS Catal* 2021, **11**: 6596–6601, https://doi.org/10.1021/acscatal.1c01128.

32. Kolb MJ, Loffreda D, Sautet P, Calle-Vallejo F: **Structure-sensitive scaling relations among carbon-containing species and their possible impact on CO2 electroreduction**. *J Catal* 2021, **395**, https://doi.org/10.1016/j.jcat.2020.12.026.

33. Calle-Vallejo F, Koper MTM: **Theoretical considerations on the electroreduction of CO to C2 Species on Cu(100) electrodes**. *Angew Chem Int Ed* 2013:52, https://doi.org/10.1002/anie.201301470.

34. Piqué O, Low QH, Handoko AD, Yeo BS, Calle-Vallejo F: **Selectivity map for the late stages of CO and CO2 reduction to C2 species on copper electrodes**. *Angew Chem Int Ed* 2021: 60, https://doi.org/10.1002/anie.202014060.

35. Kresse G, Furthmüller J: **Efficient iterative schemes for ab initio total-energy calculations using a plane-wave basis set**. *Phys Rev B* 1996, **54**:11169–11186, https://doi.org/10.1103/PhysRevB.54.11169.

36. Perdew JP, Burke K, Ernzerhof M: **Generalized gradient approximation made simple**. *Phys Rev Lett* 1996, **77**: 3865–3868, https://doi.org/10.1103/PhysRevLett.77.3865.

37. Kresse G, Joubert D: **From ultrasoft pseudopotentials to the projector augmented-wave method**. *Phys Rev B* 1999, **59**: 1758–1775, https://doi.org/10.1103/PhysRevB.59.1758.

38. Urrego-Ortiz R, Builes S, Calle-Vallejo F: **Impact of intrinsic density functional theory errors on the predictive power of nitrogen cycle electrocatalysis models**. *ACS Catal* 2022, **12**: 4784–4791, https://doi.org/10.1021/acscatal.1c05333.

39. Urrego-Ortiz R, Builes S, Calle-Vallejo F: **Fast correction of errors in the DFT-calculated energies of gaseous nitrogen-containing species**. *ChemCatChem* 2021, **13**, https://doi.org/10.1002/cctc.202100125.

40. Granda-Marulanda L, Rendón-Calle A, Builes S, Illas F, Koper MTM, Calle-Vallejo F: **A semiempirical method to detect and correct DFT-based gas-phase errors and its application in electrocatalysis**. *ACS Catal* 2020, **10**:6900–6907, https://doi.org/10.1021/acscatal.0c01075.

41. Nørskov JK, Rossmeisl J, Logadottir A, Lindqvist L, Kitchin JR, Bligaard T, Jónsson H: **Origin of the overpotential for oxygen reduction at a fuel-cell cathode**. *J Phys Chem B* 2004, **108**: 17886–17892, https://doi.org/10.1021/jp047349j.

42. Rendón-Calle A, Builes S, Calle-Vallejo F: **Substantial improvement of electrocatalytic predictions by systematic assessment**

of solvent effects on adsorption energies. *Appl Catal B Environ* 2020, **276**, https://doi.org/10.1016/j.apcatb.2020.119147.

43. Romeo E, Illas F, Calle-Vallejo F: **Evaluating adsorbate–solvent interactions: are dispersion corrections necessary?** *J Phys Chem C* 2023, **127**:10134–10139, https://doi.org/10.1021/acs.jpcc.3c02934.

44. Calle-Vallejo F, Krabbe A, García-Lastra JM: **How covalence breaks adsorption-energy scaling relations and solvation restores them**. *Chem Sci* 2016, **8**, https://doi.org/10.1039/C6SC02123A.

45. ** Sargeant E, Illas F, Rodríguez P, Calle-Vallejo F: **On the shifting peak of volcano plots for oxygen reduction and evolution**. *Electrochim Acta* 2022, **426**, 140799, https://doi.org/10.1016/j.electacta.2022.140799.
Scaling relations are affected by DFT errors in gas-phase compounds. Hence, correction of these errors is necessary to obtain accurate activity/selectivity trends by means of scaling relations, catalytic matrices, and volcano plots. See also ref. [38]

46. Rendón-Calle A, Low QH, Hong SHL, Builes S, Yeo BS, Calle-Vallejo F: **How symmetry factors cause potential- and facet-dependent pathway shifts during CO2 reduction to CH4 on Cu electrodes**. *Appl Catal B Environ* 2021, **285**, https://doi.org/10.1016/j.apcatb.2020.119776.

47. Patel AM, Vijay S, Kastlunger G, Nørskov JK, Chan K: **Generalizable trends in electrochemical protonation barriers**. *J Phys Chem Lett* 2021, **12**:5193–5200, https://doi.org/10.1021/acs.jpclett.1c00800.

48. Shin S, Choi H, Ringe S, Won DH, Oh H, Kim DH, Lee T, Nam D, Kim H, Choi CH: **A unifying mechanism for cation effect modulating C1 and C2 productions from CO2 electroreduction**. *Nat Commun* 2022, **13**:5482, https://doi.org/10.1038/s41467-022-33199-8.

49. Hussain J, Jónsson H, Skúlason E: **Calculations of product selectivity in electrochemical CO2 reduction**. *ACS Catal* 2018, **8**:5240–5249, https://doi.org/10.1021/acscatal.7b03308.

50. Chen LD, Urushihara M, Chan K, Nørskov JK: **Electric field effects in electrochemical CO2 reduction**. *ACS Catal* 2016, **6**:7133–7139, https://doi.org/10.1021/acscatal.6b02299.

51. Miller SD, İnoğlu N, Kitchin JR: **Configurational correlations in the coverage dependent adsorption energies of oxygen atoms on late transition metal fcc(111) surfaces**. *J Chem Phys* 2011, **134**, 104709, https://doi.org/10.1063/1.3561287.

52. Xu Z, Kitchin JR: **Probing the coverage dependence of site and adsorbate configurational correlations on (111) surfaces of late transition metals**. *J Phys Chem C* 2014, **118**:25597–25602, https://doi.org/10.1021/jp508805h.

53. Calle-Vallejo F, Loffreda D, Koper MTM, Sautet P: **Introducing structural sensitivity into adsorption-energy scaling relations by means of coordination numbers**. *Nat Chem* 2015, **7**, https://doi.org/10.1038/nchem.2226.

54. Koper MTM: **Thermodynamic theory of multi-electron transfer reactions: implications for electrocatalysis**. *J Electroanal Chem* 2011, **660**:254–260, https://doi.org/10.1016/j.jelechem.2010.10.004.

55. Abild-Pedersen F, Greeley J, Studt F, Rossmeisl J, Munter TR, Moses PG, Skúlason E, Bligaard T, Nørskov JK: **Scaling properties of adsorption energies for hydrogen-containing molecules on transition-metal surfaces**. *Phys Rev Lett* 2007, **99**, 016105, https://doi.org/10.1103/PhysRevLett.99.016105.

56. Calle-Vallejo F, Martínez JI, García-Lastra JM, Abad E, Koper MTM: **Oxygen reduction and evolution at single-metal active sites: comparison between functionalized graphitic materials and protoporphyrins**. *Surf Sci* 2013, **607**, https://doi.org/10.1016/j.susc.2012.08.005.

57. Calle-Vallejo F, Martínez JI, Rossmeisl J: **Density functional studies of functionalized graphitic materials with late transition metals for oxygen reduction reactions**. *Phys Chem Chem Phys* 2011, **13**, https://doi.org/10.1039/c1cp21228a.